OPTIMIZATION OF LINEAR INDUCTION RADIGRAPHY ACCELERATOR WITH ELECTRON BEAM WITH ENERGY VARIATION

Lawrence Livermore National Laboratory

Yuan Hui Wu and Yu-Jiuan Chen

Lawrence Livermore National Laboratory

ENGINEERING

Abstract

The current interest for the next generation linear induction radiography accelerator (LIA) is to generate multiple electron beam pulses with high peak currents. The beam energy and current may vary from pulse to pulse. Consequently, the transport and control of multi-pulsing intense electron beams through a focusing lattice over a long distance on such machine becomes challenging. Simulation studies of multi-pulse LIAs using AMBER [1] and BREAKUP Code [2] are described. These include optimized focusing magnetic tune for beams with energy and current variations, and steering correction for corkscrew motion. The impact of energy variation and accelerating voltage error on radiograph performance are discussed.

Introduction

Controlling beam transport is essential for accelerator operation and future induction accelerator design. In this study, see Figure 1, we simulated a conceptual linear induction accelerator. The nominal incoming 2-MeV, 2-kA electron beam exiting from the diode injector has a uniform KV distribution with a 5 cm edge radius (r = 5 cm) and a 800π mm-mrad edge normalized emittance ($\varepsilon = 800\pi$ mm-mrad). The incoming beam has a small energy variation (dg/g), which varies from -5% to 5% with respect to the nominal beam energy.

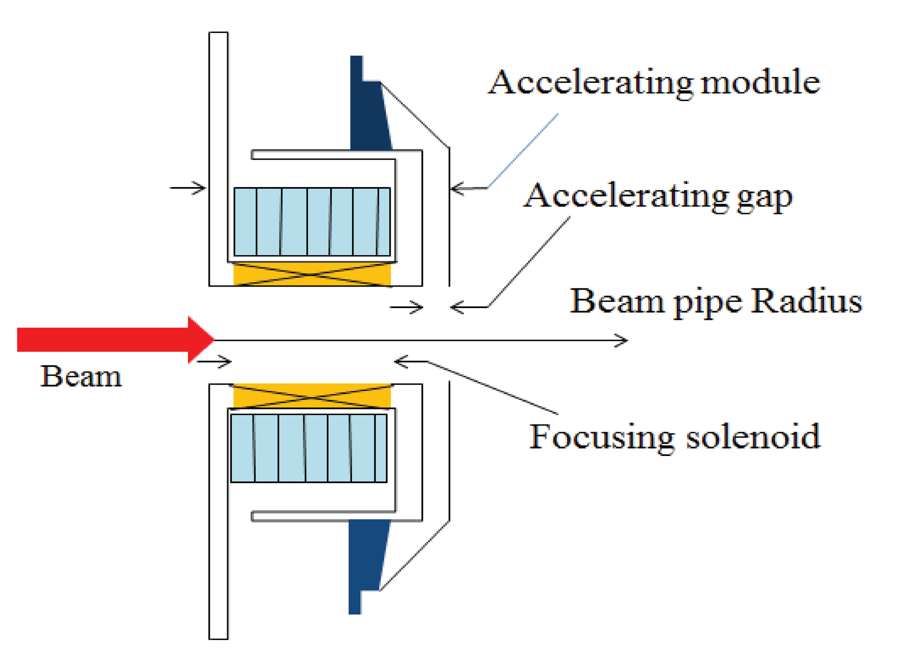

Figure 1: Schematic of simulated 250kV accelerating cell.

Contact Information

Yuan Hui Wu
Lawrence Livermore National Laboratory
wu39@llnl.gov
925-423-4981

Conceptual Accelerator Configuration

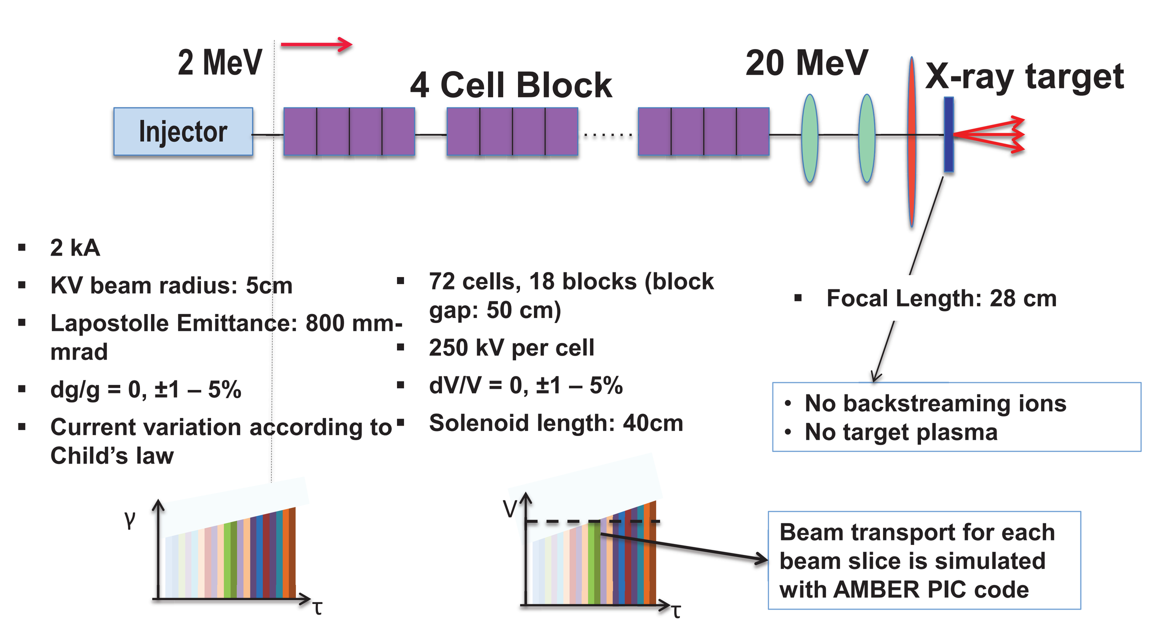

Electron Beam Transport and Tune Optimization

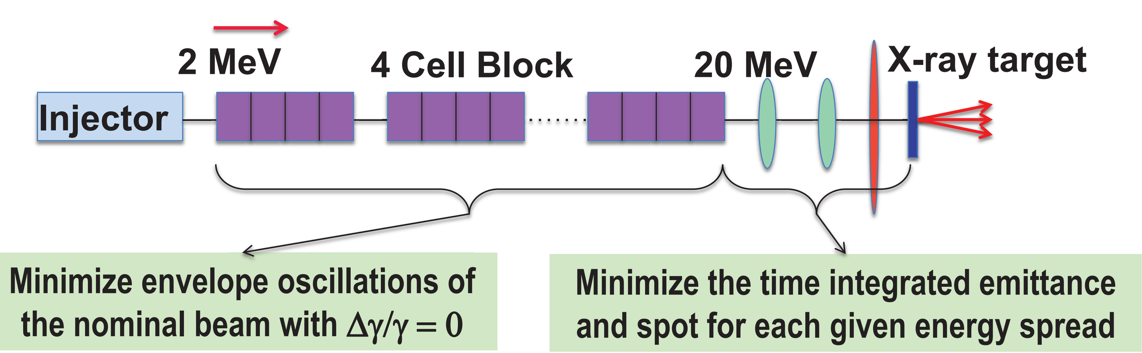

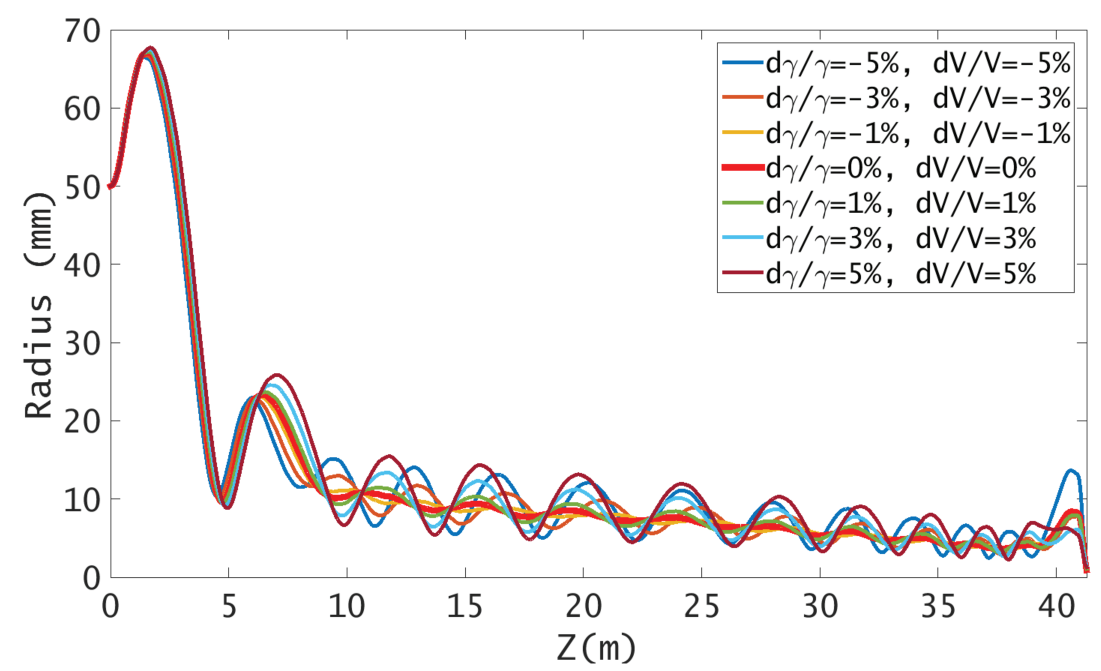

Figure 2: Envelopes for electron beam with different initial energy variation dg/g and accelerating voltage error dV/V. The beam envelope for the nominal beam is given by the thick red line.

Electron Beam at the Accelerator Exit

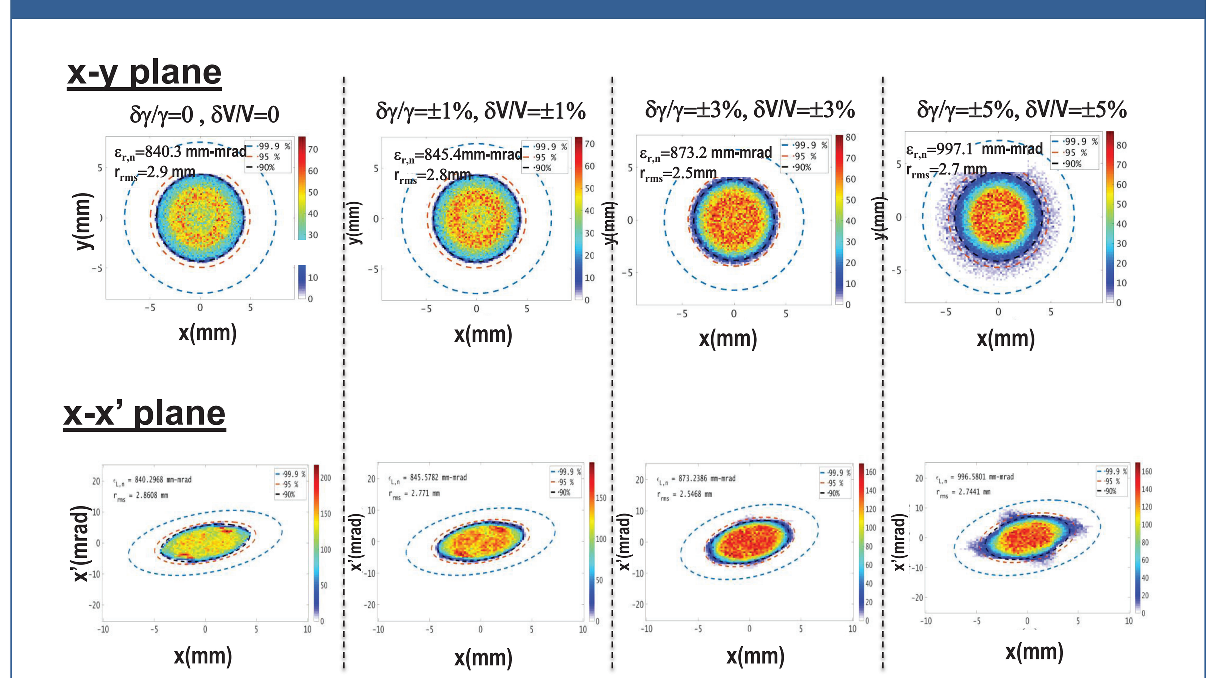

Figure 3: the beam size and emittance of the beam at the accelerator exit increase for the beam pulse with a larger initial energy variation or for a larger accelerating voltage error.

Final Focus Optimization

- Multi-Objectives Global optimization algorithm (Genetic Algorithm) [4] is used to optimize the magnetic setting for minimum integrated emittance and the desired time integrated spot sizes at the target (Figure 5).

$$R_f^2 \approx \left(\frac{\varepsilon f}{R_i}\right)^2 + (R_i' f)^2 + \left(2\frac{\delta\gamma}{\gamma}R_i\right)^2 + \left(\frac{C_s R_i^3}{4}\right)^2 + \left(\frac{\delta I}{I}F(R_i)\right)^2$$

envelope divergence, spherical aberration, emittance, chromatic aberration, space-charge

Scaling law for final spot size [5]

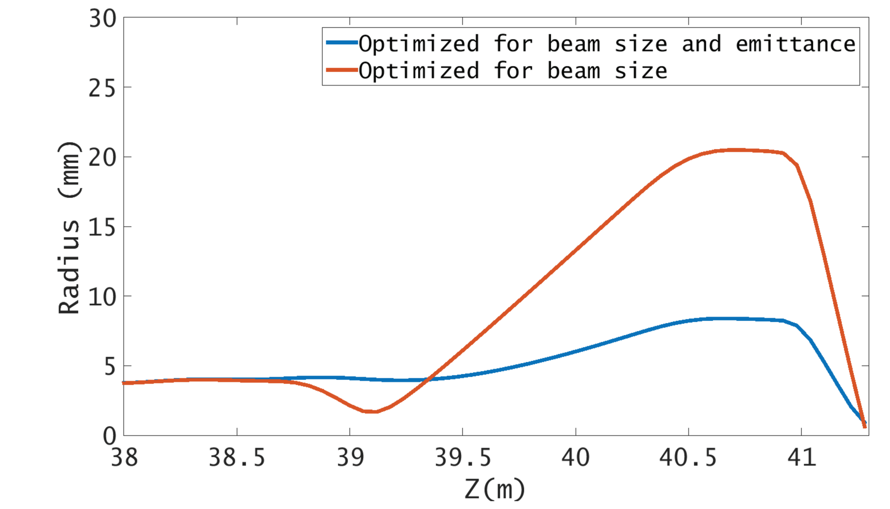

Figure 4: Beam envelopes can be chosen for the smallest possible spot with emittance growth (red) or for a 1.2-mm MTF spot while preserving the emittance (red)

Electron Beam at the Target

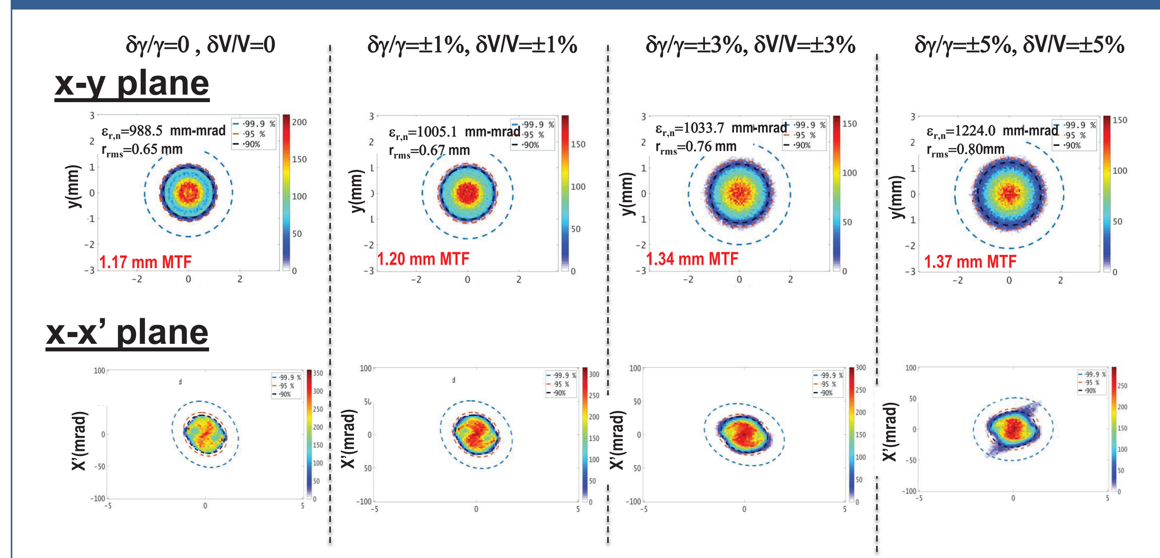

Figure 5: the beam size and emittance of the beam at the accelerator exit increase for the beam pulse with a larger initial energy variation or for a larger accelerating voltage error.

Injector energy spread $\delta\gamma/\gamma$ (± %)	Accelerator Voltage variation $\delta V/V$ (± %)	R_{rms} (mm)	Normalized Lapostolle Emittance (mm-mrad)	50% MTF (mm)	ΔD/D (%)
0	0	0.65	988	1.17	0
1	1	0.67	1005	1.20	0.2
2	2	0.72	1026	1.25	1.0
3	3	0.76	1034	1.34	1.8
5	5	0.80	1224	1.37	0.6

Table 1: The radiography resolution depends on the spot size defined by the 50% modulation transfer function (MTF) [7]. We used the time-integrated profiles to calculate the 50% MTF spot sizes for all the cases we studied, which are shown in Table 1. Both the initial energy spread and the accelerating voltage error have large impact on the 50% MTF spot size.

Corkscrew Motion Minimization

- Corkscrew motion is caused by misalignment and chromatic aberration of the transport system
- Beam centroid (z,t) gyrates around the offset flux line
  - the gyro-radius $|r(z,t)| \propto (dB/B)_{kc}$
  - The flux line displacement $D(z) \propto (dB/B)_{k=0}$

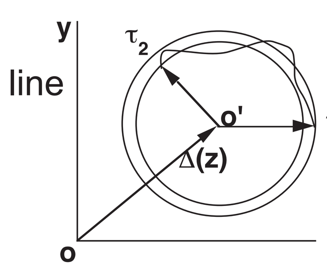

- Corkscrew amplitude A(z)

$$|A|^2(z) = \langle (x(z,t) - \langle x(z,t)\rangle)^2 \rangle + \langle (y(z,t) - \langle y(z,t)\rangle)^2 \rangle \propto |r(z,t)|^2$$

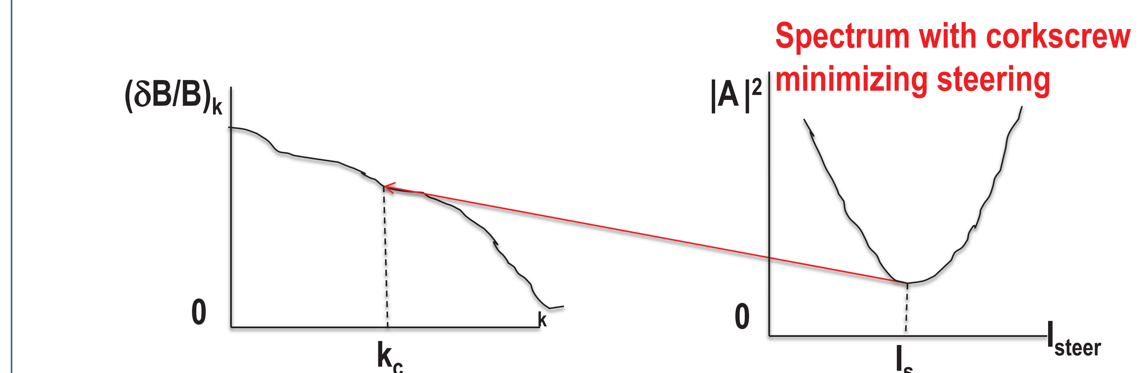

Figure 6: Minimizes the error field's k_c components for beam slices over a range of energy/time

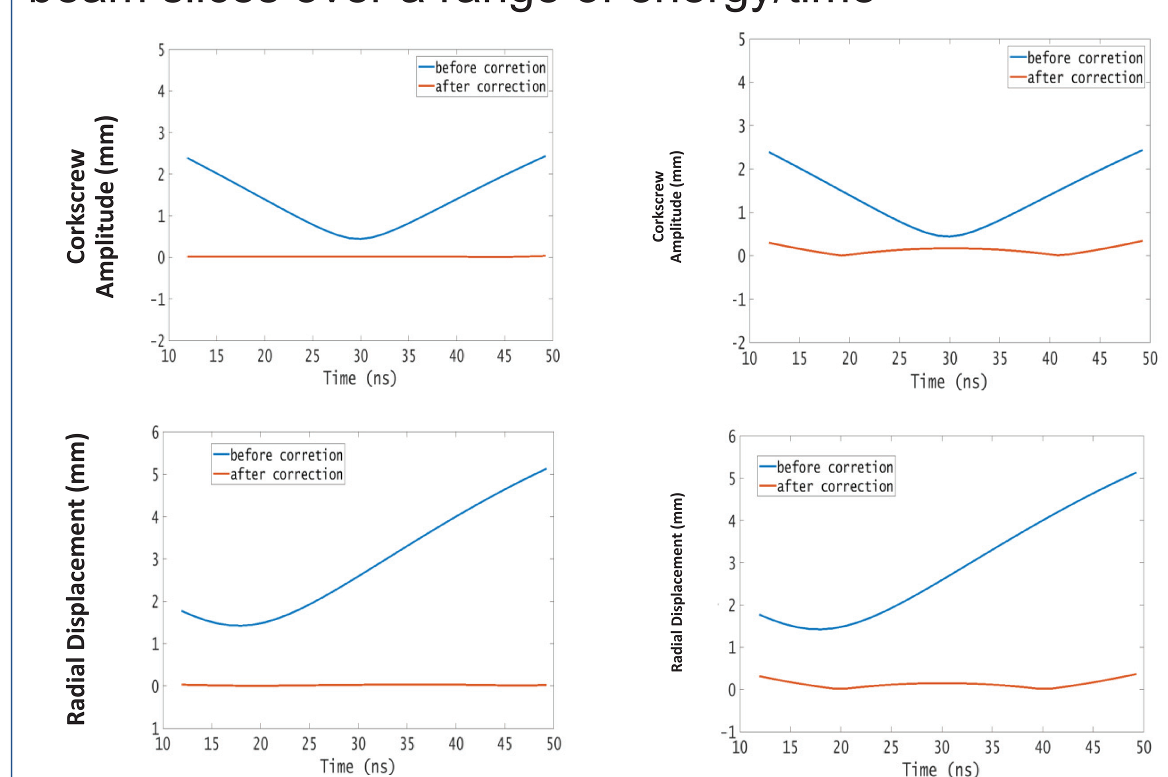

Figure 7:corkscrew motion and the central displacement. Solenoid magnets were randomly misaligned with solenoid displacement 3s = 2 mm and solenoid tilt 3s = 2 mrad. The accelerator voltage error dV/V is ±5%. The beam's initial dg/g is ± 5%, and its initial offset $x_{off} = y_{off} = 0.5$ mm.

Conclusions

Beam transport on a conceptual induction accelerator was optimized with Global optimization algorithm. The effect of energy variation of electron beam on the radiography performance was evaluated. Energy variation has large impact on the 50% MTF spot size but not on the forward x-ray dose. The optimization scheme can also be used to set the magnetic strength of two steering coil pairs to reduce corkscrew motion and transverse centroid displacement.

Reference

[1] J. L. Vay, W. Fawley, Amber code, 2000
[2] Y.-J Chen, W. Fawley, BREAKUP Code
[3] M. Reiser, Theory and design of charged particle beams, New York. NY: Wiley, 1994 [4]
[4] K. Deb. John Wiley and Sons, Chichester, 2001.
[5] G. J. Caporaso and Y.-J Chen, UCRL-JC-130594, LLNL
[6] Y. Wu, Y-J. Chen, napac conference, 2016.
[7]C. Ekdahl, Vol. 28, No. 12, J. Opt. Soc. Am.
[8] Y.-J Chen, April 2000. UCRL-ID-140189, LLNL
[9] Y.-J. Chen, Nucl. Inst. Meth. A, 398:139, 1997.